Supporting Information

Stern et al. 10.1073/pnas.1420932112

SI Text

SAM Experiments

MTBSTFA Reduction Methods. During the first EGA experiments at RN, contributions from the terrestrial derivatization reagents [*N*-methyl-*N*-*tert*-butyldimethylsilyl-trifluoroacetamide (MTBSTFA) and dimethylformamide (DMF)] carried for SAM's derivatization experiment to the SAM background were identified (1, 2). Several strategies were devised to minimize volatile contributions from MTBSTFA and its reaction products during the experiments conducted on the JK and CB drill hole samples (Table S1). At JK, samples were preheated to 320 °C (JK-Blank to JK-3) for ∼20 min ("boil-off") to remove MTBSTFA and its by-products. A second MTBSTFA reduction experiment developed for the CB-5, CB-6, CB-6–residue, CB-7, and CB-Blank2 experiments, consisted of (*i*) pumping out the Sample Manipulation System (SMS) for ∼3 h with venting to the atmosphere via the wide-range pump before receiving sample, with the SAM gas manifolds and transfer lines heated to 135 °C; (*ii*) flushing the pyrolysis oven and SMS with helium to minimize adsorption of MTBSTFA products inside the oven; and (*iii*) preheating the selected cup for ∼20 min to ∼200 °C (CB-5) or ∼250 °C (CB-6, CB-6–residue, CB-7, and CB-Blank2) before moving the cup under the inlet tube to receive its portion of the solid sample (for triple samples, this results in the first two portions delivered being heated to ∼200 °C). However, in addition to removing MTBSTFA and its by-products from the sample during these procedures, information on many low-temperature volatile species in the sample was also lost. Due to these variations in sample handling (Table 1 and *SI Text*), samples CB-6 and CB-7 contain lower abundances of all volatiles than RN, JK, or other CB samples. In CB-6 and -7, three portions of sample were deposited into a hot cup (∼250 °C), driving off a significant amount of all N species before the sample analysis. The calculated abundances of N-bearing species are included for completeness but are expected to differ from previous CB runs because of the way the samples were handled before analysis.

CB-6–Reheat Experiment. An experiment was performed to test adsorption of MTBSTFA onto an already pyrolyzed sample, CB-6. In the CB-6–reheat experiments, CB-6 was reexposed to the sample carousel, where it would have come into contact with MTBSTFA vapor, and resulted in the same abundances of reduced species HCN and TFMA as the original CB-6 sample, suggesting that some portion of HCN, like TFMA, is formed as a by-product of the decomposition of MTBSTFA (although this does not exclude the possibility of a martian contribution). Reheating of the CB-6 sample produced approximately seven times less NO than the original CB-6 sample (Table 1, main text), arguing for a martian source for the bulk of the NO evolved in CB-6. In addition, the behavior of HCN (and ClCN) at RN, JK, and CB is remarkably consistent, characterized by a sharp, narrow peak at ∼275 °C, whereas there is considerable site-to-site variation in the NO release profile (Fig. 1, main text). Furthermore, there appear to be multiple NO releases in each martian sample, evidenced by peaks at different temperatures, suggesting that even if there is a low-temperature NO release associated with the decomposition of terrestrial contaminants, other martian sources of NO are also present.

Methods for N-Bearing Compound Identification and Quantification. SAM GCMS experimental data were used primarily for molecular identification of nitrogen-bearing species. GCMS analysis provides two complementary pieces of data specific to a given chemical species: compound retention time and the mass fragmentation patterns obtained from the QMS. For compound identification, SAM QMS fragmentation patterns are compared with the National Institute of Standards and Technology (NIST) reference mass spectral library (Fig. S2). Several of the nitrogen-bearing species are poorly retained on the GC analytical column (GC-5-MXT CLP, polydimethylsiloxane with phenyl and cyanopropyle) used for all analyses, as this channel is targeted to separate medium-weight organic molecules (C5–C15). This results in the coelution of most of the nitrogen-bearing molecules in a large peak of multiple masses early in the GC run. Molecules such as HCN [primary ions mass-to-charge ratio (*m*/*z*) 26 and 27] and possibly ammonia (primary ions *m*/*z* 16 and 17) that have diagnostic masses with possible contributions from other species such as H_2O, CH_4, and other hydrocarbons fragments posed additional challenges for their identification by GCMS. For HCN, *m*/*z* 26/27 ratios from EGA-QMS were used to identify HCN. However, the presence and abundance of ammonia is difficult to demonstrate with EGA data due to mass interferences at *m*/*z* 15, 16, and 17, ions that can be attributed to methyl groups, oxygen, and water. Efforts to use SAM data to estimate ammonia abundance have been undertaken and upper limits were calculated for RN, assuming no contribution from *m*/*z* 15 by CH_3 (3, 4). However, without GCMS confirmation, it is not possible to make a definitive detection or estimate of NH_3.

Acetonitrile (CH_3CN) was identified in GCMS data but not in EGA data due to its primary ion fragment, *m*/*z* 41, being the same as 2-methylpropene (C_4H_6), which is present at 1–2 orders of magnitude higher abundance. It is also possible that CH_3CN is being made in the GC trap from trifluoroacetonitrile (TFA, CF_3CN), which is identified in both EGA and GC. Because TFA shares several characteristic ion fragments with other chemical species present in these runs (e.g., 69 from trichloromethane; 76 from CS_2), its abundance was estimated from integration of *m*/*z* 76 <500 °C, where contribution from CS_2 is not present.

The assignment of NO to *m*/*z* 30 was based on the matching of the *m*/*z* 31/30 ratio in SAM data to NIST ratios (Figs. S2 and S3). Other possible contributions to *m*/*z* 30 include formaldehyde (CH_2O) and ethane, which both have a strong ion fragment contribution at *m*/*z* 29 and are decomposition products of MTBSTFA/DMF. However, in SAM GCMS data, the *m*/*z* 29 and 30 peaks have different retention times, with *m*/*z* 30 eluting before *m*/*z* 29 (Fig. S4). If *m*/*z* 29 is from CH_2O, its abundance is consistent over both sample (CB-5) and blanks (CB-Blank2, CB-6–residue, treated as a blank for most species including NO), whereas there is clearly more NO in samples than blanks. Based on GCMS data for runs where gas evolved at comparable temperatures is sent to the GC, *m*/*z* 30 estimated from *m*/*z* 29 peak area and inferred from the NIST CH_2O 29/30 ratio accounts for ∼2% of the total *m*/*z* 30 peak. Because the error on our EGA quantification is ∼20%, for the purposes of quantification, we can treat all of the *m*/*z* 30 as if it is coming from NO.

EGA-QMS data were used to quantify nitrogen species and MTBSTFA/DMF-derived products using the same procedures detailed in previous publications (1, 5). To summarize, dead-time corrections for QMS intensity were made based on data acquired

during preflight calibration of the SAM flight model (FM) (6). Abundances for chemical species were calculated by integrating the peak areas for the diagnostic ion fragments for each species of interest, extrapolating to the total peak areas computed from the NIST ratio of all *m/z* values that contribute to >10% of the base peak (see Table S2 for *m/z* values used) and correcting for ionization cross-section differences relative to CO_2. The abundances were computed by referencing the corrected total ion counts to a moles/counts ratio for *m/z* 44 derived during prelaunch EGA calibrations on the SAM FM where CO_2 was evolved from a known quantity of a calcite standard a moles/counts per second ratio of $2.72 \times 10^{-15} \pm 1.5 \times 10^{-16}$ for *m/z* 44 derived from ref. 3. An error of 20% is based upon (*i*) the moles/counts ratio for *m/z* 44, (*ii*) variation of ionization cross-sections in the literature, and (*iii*) at what time/temperature during the pyrolysis run background was selected for subtraction from the total QMS signal. For additional details on the QMS scan mode, the SAM data analysis software, the EGA quantification, see Mahaffy et al. (7), Leshin et al. (1), Franz et al. (6), and Ming et al. (5).

Laboratory Experiments

EGA-QMS. When fragments characteristic of the terrestrial derivatization reagent *N*-methyl-*N*-*tert*-butyldimethylsilyl-trifluoroacetamide (MTBSTFA) carried for SAM's derivatization experiment were found in the first SAM EGA analyses of RN, laboratory EGA experiments were performed on samples containing MTBSTFA and calcium perchlorate to better understand the decomposition and oxidation of MTBSTFA under SAM experimental conditions. Masses associated with all of the N compounds detected by SAM EGA are detected in laboratory experiments performing EGA on fused silica doped with MTBSTFA (Fig. S4). Laboratory EGA tests were performed on a Frontier Autoshot-Py3030 pyrolyzer attached to an Agilent 7890A gas chromatograph (GC)–5975C inert XL mass spectrometer detector (MSD). The pyrolyzer was initially held at 50 °C for 25 min and ramped at 35 °C/min to 1,050 °C where it was held for 5 min. Inert pyrolysis under 30 mbar of helium generated evolved gases that were split at a ratio of 10:1 and carried with 0.5-sccm helium flow through the inlet, column, and transfer line, all held at an isotherm of 135 °C, to the MSD. The MSD scanned 2–535 Da. Samples consisted of fused silica (HP Technical Ceramics; FS-120; for details, see ref. 8) doped with 1 wt % $Ca(ClO_4)_2 \bullet nH_2O$ (Sigma-Aldrich, 99% purity) and small volumes of MTBSTFA (Sigma-Aldrich; 97% purity) and DMF (Sigma-Aldrich; 99.8% purity). Masses consistent with N-bearing species identified in SAM EGA were thermally evolved before the onset of the oxygen peak (Fig. S5). The primary decomposition product was TFMA, with smaller amounts of *m/z* 26, 27, 30, 41, and 61 possibly associated with HCN, ClCN, 2-methylpropene, and NO.

EGA experiments to observe the thermal decomposition of calcium nitrate tetrahydrate [$Ca(NO_3)_2 \bullet 4H_2O$; Sigma], iron(III) nitrate nonahydrate [$Fe(NO_3)_3 \bullet 9H_2O$; Sigma], and magnesium nitrate hexahydrate [$Mg(NO_3)_2 \bullet 6H_2O$; Sigma] were performed on a SAM-like laboratory system consisting of an in-house pyrolysis oven coupled to a Hiden Analytical HPR-20 QMS. Samples were weighed into quartz boats and loaded into the pyrolysis oven. Samples were heated from ∼50 to ∼1,000 °C at a ramp rate of 20 °C/min, under an ∼1-sccm He flow and ∼30-mbar He pressure, and evolved gases were monitored by the QMS. A 20 °C/min ramp rate (vs. the SAM rate of 35 °C/min) was used to mitigate the impact of the relatively slow scan speed of the Hiden QMS; the slower heating rate allowed time sampling similar to that of other SAM-like EGA systems. The QMS mass range is *m/z* 1–300, but a "peak-hopping" mode was used, in which several *m/z* values of interest were monitored to achieve higher time sampling.

Pyrolysis-GCMS. Pyrolysis-GCMS (py-GCMS) experiments (Fig. S6) focused on reactions between 1 wt % $Ca(ClO_4)_2 \bullet nH_2O$ (Sigma-Aldrich; 99% purity) and small volumes of MTBSTFA (Sigma-Aldrich; 97% purity) and DMF (Sigma-Aldrich; 99.8% purity). Samples were composed of fused silica (HP Technical Ceramics; FS-120; for details, see ref. 8) and doped with Ca-perchlorate (28 mg total) with or without addition of 0.4 mL of MTBSTFA (∼1.7 mmol) + 0.1 mL of DMF (∼1.3 mmol). The py-GCMS experimental setup was customized to approximate the SAM GCMS analytical conditions. Volatile compounds released from solid samples in the Chemical Data Systems (CDS) model 5200 pyrolysis unit were transferred to the hydrocarbon trap downstream consisting of equal volumes of glass beads, 60/80 Tenax TA, and 60/80 Carbosieve G, and held cryogenically at 5 °C during the entire pyrolysis heating ramp. The He flow is then reversed from the trap to a Thermo Finnigan Trace GC split/splitless inlet while the hydrocarbon trap is ballistically heated to 300 °C and held for 4 min. Volatile compounds are transferred from the pyroprobe hydrocarbon trap to the inlet of the GC via a heated transfer line (135 °C). The GC is operated in split mode (10:1) under a constant He flow of 1.5 mL/min. The initial GC oven temperature was set to 50 °C for 4 min and then ramped at 10 °C/min to 250 °C, followed by a hold at 250 °C for 20 min. Volatile compounds released from the hydrocarbon trap were separated in the GC oven using a Restek MXT-Q-Bond column usually used in laboratory for separation of C_1–C_{14} hydrocarbons and small inorganic volatiles, and transferred to a Thermo Finnigan Trace DSQII QMS that scanned *m/z* values in the 25–350 range.

MTBSTFA Calculations

MTBSTFA was estimated using a modification of the method presented by Ming et al., who used the following products and their most diagnostic ion fragments: *tert*-butyldimethylsilanol (monosilylated H_2O, MSW) (*m/z* 75), 1,3-bis(1,1-dimethylethyl)-1,1,3,3-tetramethyldisiloxane (bisilylated H_2O, BSW) (*m/z* 147), *tert*-butyldimethylfluorosilane (TBDMS-F) (*m/z* 134), and the mole fraction of C from 2,2,2-trifluoro-*N*-methylacetamide (TFMA) (*m/z* 127) relative to the sum of the other silylated products. We have since identified two additional decomposition products of MTBSTFA: 2-methylpropene (C_4H_8) (*m/z* 41) and a strong contribution at *m/z* 15, either CH_4 or methylene ions, and include these in our calculations (Table S3). Although these products do not, themselves, contain N, they each represent a fragment of the MTBSTFA molecule, and thus a corresponding N-bearing decomposition product.

MTBSTFA-derived N calculations can be performed in two ways, both of which give the same values. Method 1 involves calculating the C contributed by each of the MTBSTFA-derived fragments above, and then ratioing this value to the MTBSTFA C:N ratio of 9:1 to obtain MTBSTFA-derived N. Method 2 involves taking into account the N contributed per MTBSTFA fragment molecule. For example, 1 BSW molecule is formed from 2 MTBSTFA fragments, each of which contributes 1 nitrogen. Using this rationale, the abundance of MTBSTFA N can be calculated using the following formula using the molar abundances of each decomposition product:

$$2 \times \mathrm{BSW} + \mathrm{MSW} + \mathrm{TBDMS\text{-}F} + \mathrm{C_4H_8} + 1/5 \times \mathrm{CH_4}.$$

1. Leshin LA, et al.; MSL Science Team (2013) Volatile, isotope, and organic analysis of martian fines with the Mars *Curiosity* rover. *Science* 341(6153): 1238937.

2. Glavin DP, et al. (2013) Evidence for perchlorates and the origin of chlorinated hydrocarbons detected by SAM at the Rocknest aeolian deposit in Gale crater. *J Geophys Res Planets* 118(10):1955–1973.

3. Archer PD, et al. (2014) Abundances and implications of volatile-bearing species from evolved gas analysis of the Rocknest aeolian deposit, Gale crater, Mars. *J Geophys Res Planets* 119(1):237–254.
4. Wray JJ, et al. (2013) The search for ammonia in martian soils with *Curiosity*'s SAM instrument. *Lunar Planet Sci XLIV* (Lunar and Planetary Institute, Houston), 2942.
5. Ming DW, et al.; MSL Science Team (2014) Volatile and organic compositions of sedimentary rocks in Yellowknife Bay, Gale crater, Mars. *Science* 343(6169):1245267.
6. Franz HB, et al. (2014) Analytical techniques for retrieval of atmospheric composition with the quadrupole mass spectrometer of the Sample Analysis at Mars instrument suite on Mars Science Laboratory. *Planet Space Sci* 96:99–113.
7. Mahaffy P, et al. (2012) The Sample Analysis at Mars investigation and instrument suite. *Space Sci Rev* 170(1-4):401–478.
8. Conrad PG, et al. (2012) The Mars Science Laboratory organic check material. *Space Sci Rev* 170(1-4):479–501.

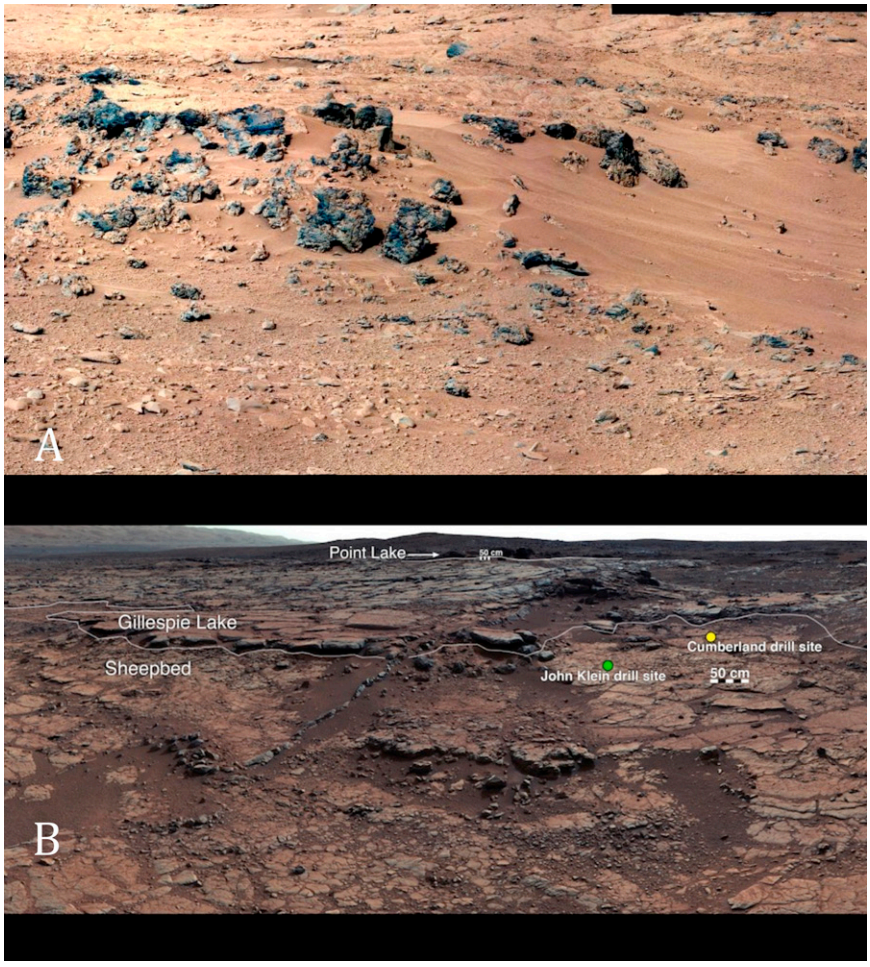

Fig. S1. (*A*) Rocknest (RN) is an aeolian deposit consisting of fine-grained material with a bulk composition similar to martian fines previously characterized at other locations on Mars. Samples were scooped and then sieved to <150 μm before delivery to the SAM instrument. Image courtesy of National Aeronautics and Space Administration (NASA)/Jet Propulsion Laboratory (JPL)–Caltech/Malin Space Science Systems (MSSS). (*B*) Location of John Klein (JK) and Cumberland (CB) drill sites in the Sheepbed mudstone member of Yellowknife Bay. Image courtesy of NASA/JPL-Caltech/MSSS.

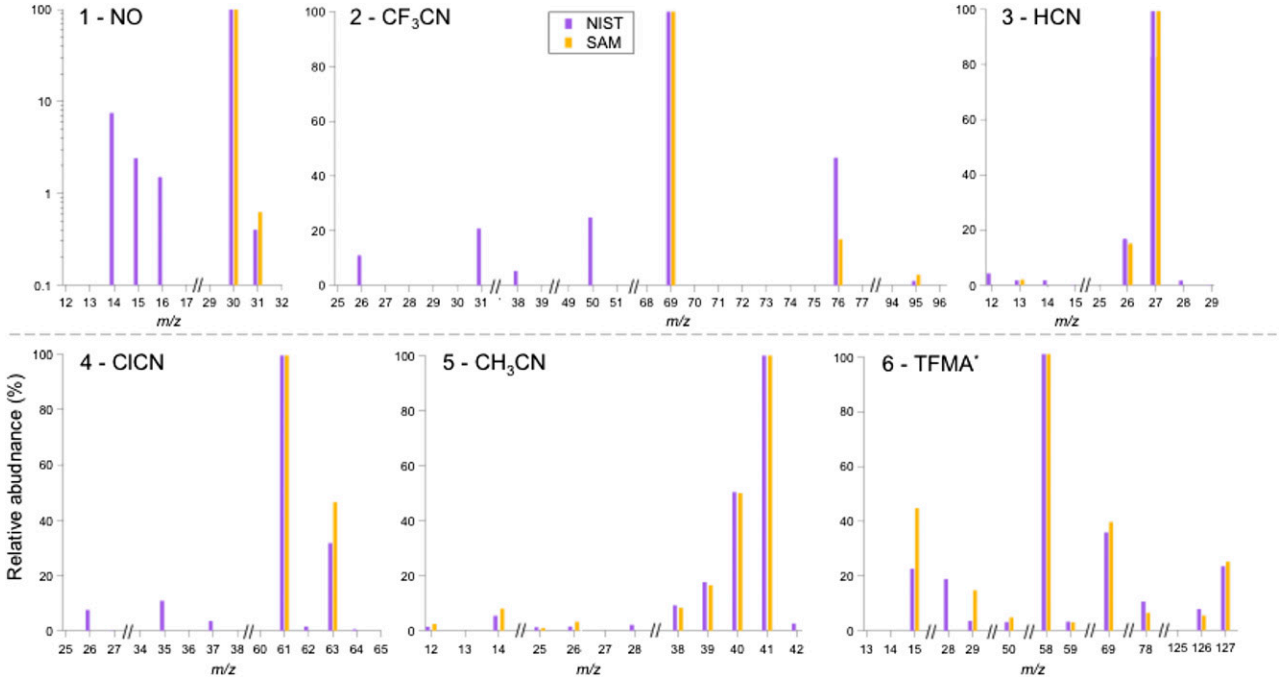

Fig. S2. Mass-spectral identifications of NO, CF_3CN, HCN, ClCN, CH_3CN, and TFMA from SAM GCMS compared with NIST library spectra.

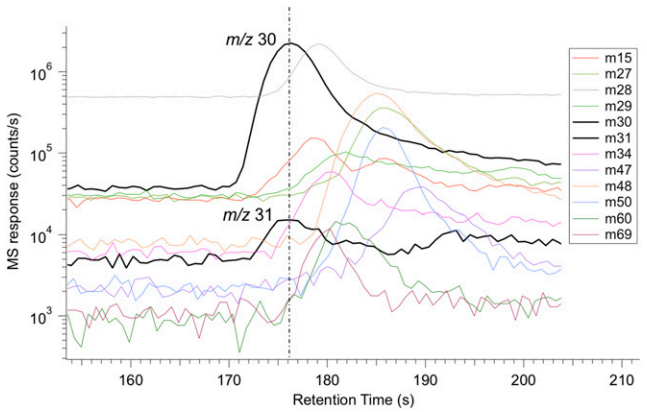

Fig. S3. GC chromatogram (log scale) highlighting the coelution of *m/z* 30 and *m/z* 31 at ratios consistent with NO. The NO peak elutes before a peak of poorly retained compounds with coeluting masses that are hard to resolve from one another.

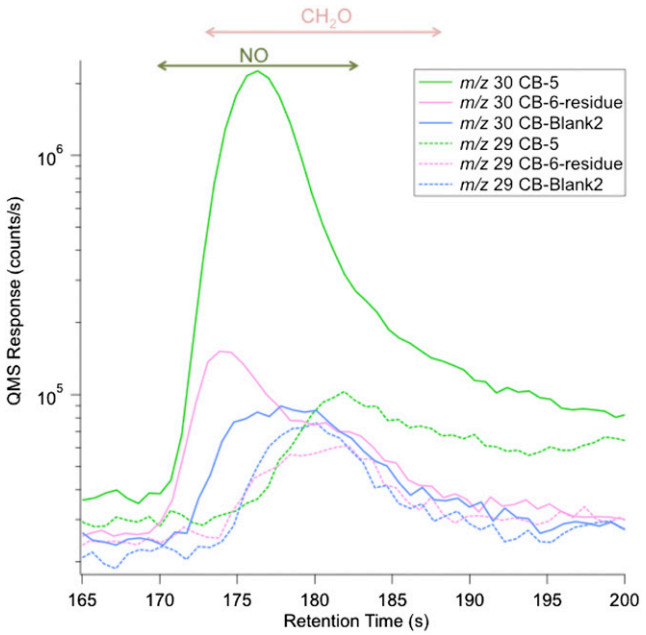

Fig. S4. Traces showing different retention times for *m/z* 30 and *m/z* 29 during sample (CB-5) and blank (CB-Blank2, CB-6–residue). This supports the identification and quantification of *m/z* 30 as NO, and not formaldehyde.

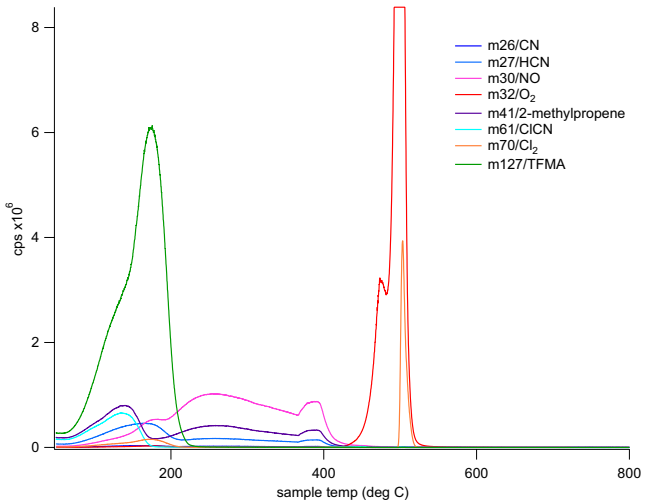

Fig. S5. Laboratory EGA experiments with MTBSTFA and Ca-perchlorate—the major N-bearing product of MTBSTFA decomposition in these experiments is TFMA. All species are evolved before the onset of oxygen release from perchlorates at ~425 °C. Smaller amounts of HCN, NO, and ClCN are released; however, these species are less abundant with respect to TFMA than what we see in SAM-EGA samples at RN, JK, and CB.

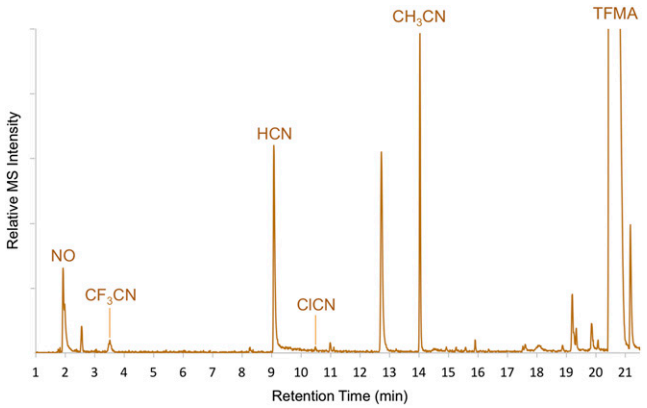

Fig. S6. Detection of N species in py-GCMS experiments with MTBSTFA, DMF, and 1% perchlorate on fused silica.

Table S1. Analytical protocol for SAM-EGA-QMS and GC-QMS analyses

Drill hole target	Sample no.	Analysis on Mars, Sol no.	EGA–pyrolysis temperature*	GC hydrocarbon trap cut[†]
Rocknest (RN)	RN-Blank		Continuous temperature ramp, ~45–875 °C	
	RN-1	93	Continuous temperature ramp, ~45–875 °C	146–533 °C
	RN-2	96	Continuous temperature ramp, ~45–875 °C	98–425 °C
	RN-3	99	Continuous temperature ramp, ~45–875 °C	533–822 °C
	RN-4	117	Continuous temperature ramp, ~45–875 °C	252–289 °C
John Klein (JK)	JK-Blank	177	Boil-off to 300 °C; temperature ramp, ~300–881 °C	314–822 °C
	JK-1	196	Boil-off to 300 °C; temperature ramp, ~300–881 °C	314–822 °C
	JK-2	199	Boil-off to 300 °C; temperature ramp: ~300–881 °C	245–643 °C
	JK-3 (3× portion)	224	Boil-off to 300 °C; temperature ramp, ~300–881 °C	245–643 °C
	JK-4	227	Continuous temperature ramp, ~45–875 °C	574–797 °C
Cumberland (CB)[‡]	CB-Blank1	277	Continuous temperature ramp, ~45–875 °C	445–548 °C
	CB-1	282	Continuous temperature ramp, ~45–875 °C	445–548 °C
	CB-2	286	Continuous temperature ramp, ~45–875 °C	574–797 °C
	CB-3	290	Continuous temperature ramp, ~45–875 °C	229–350 °C
	CB-5	368	MTBSTFA reduction[§]; temperature ramp, ~45–875 °C	229–350 °C
	CB-6 (3× portion)	382	MTBSTFA reduction[§]; temperature ramp, ~250–870 °C	229–350 °C
	CB-6 residue[¶]	394	MTBSTFA reduction[§]; temperature ramp, ~250–870 °C	229–350 °C
	CB-7 (3× portion)	408	MTBSTFA reduction[§]; temperature ramp, ~250–870 °C	496–797 °C
	CB-Blank2	421	MTBSTFA reduction[§]; temperature ramp, ~250–870 °C	496–797 °C

*The sample preheat temperatures are determined from thermocouple measurements of fused silica powder heated in a SAM flight spare oven using the same power profile as the SAM flight oven.

[†]Gas chromatography (GC) hydrocarbon trap cut refers to the cup temperature range over which volatiles were collected on the hydrocarbon trap during pyrolysis for GCMS analyses.

[‡]The details for CB-4 were not included because this experiment was an EGA noble gas enrichment experiment that is not discussed in this paper.

[§]The MTBSTFA reduction experiment used in the CB-5, CB-6, CB-6 residue, CB-7, and empty cup CB-Blank2 analyses included a pump-out of the Sample Manipulation System (SMS) and preheating of the sample cup in the pyrolysis oven to >200 °C (CB-5) or >250 °C (CB-6, CB-6 residue, CB-7, and CB-Blank2) before receiving each sample portion from *Curiosity*'s sample delivery system. Because no sample was delivered to the cups for the CB-6 residue and CB-Blank2 experiments, a "fake" sample handoff was carried out before pyrolysis to simulate the same sample exposure conditions inside the SMS for both single- and triple-portion solid-sample analyses. These experiments also included an additional sample preheat for 20 min to >45 °C for CB-5 and >250 °C for CB-6, CB-6 residue, CB-7, and the CB-Blank2 before the 35 °C/min pyrolysis temperature ramp.

[¶]The CB-6 triple-portion sample residue was pyrolyzed and analyzed a second time using the identical experimental conditions that were used for the CB-6 triple-portion run.

Table S2. Values used to calculate abundance of target chemical species

Value	HCN, nmol	NO, nmol	ClCN, nmol	TFA, nmol	TFMA, nmol
m/z values used for abundances*	26, 27	30	35, 61, 63	12, 26, 38, 50, 69, 76	15, 28, 58, 69, 78, 127
Ratio of ionization cross-section (CO_2/N compound)†	44/27 = 0.58	44/30 = 1.32	44/61 = 1.03	44/76 = 0.59	44/127 = 0.23

Abundances for chemical species were calculated by integrating the peak areas for the diagnostic ion fragments for each species of interest, extrapolating to the total peak areas computed from the NIST ratio of all *m/z* values that contribute to >10% of the base peak, and correcting for ionization cross-section differences relative to CO_2. Underlined number represents the major ion fragment used for detection and calculation of species abundance.

**m/z* ratios from NIST database.

†The ionization cross-sections at 70 or 75 eV of the compounds of interest were obtained and cross-compared between the NIST database, published literature, and calculations from bond contributions. Variation between ICS from different sources is ~13% and is factored into error calculations.

Table S3. Decomposition products detected during SAM EGA analysis

Run	BSW, nmol	MSW, nmol	TBDMS-F, nmol	C_4H_8, nmol	CH_4, nmol	TFMA, nmol	MTBSTFA total N,* nmol N
RN-Blank	3.9 ± 0.8	0.2 ± 0.0	0.7 ± 0.1	18 ± 4	109 ± 22	0	49 ± 10
RN-1	2.4 ± 0.5	0.8 ± 0.2	0.5 ± 0.1	26 ± 5	108 ± 22	<1	54 ± 11
RN-2	2.4 ± 0.5	1.3 ± 0.3	0.8 ± 0.2	44 ± 9	141 ± 28	1.3 ± 0.3	79 ± 16
RN-3	2.3 ± 0.5	1.1 ± 0.2	0	39 ± 8	127 ± 25	1.9 ± 0.4	70 ± 14
RN-4	2.9 ± 0.6	0.7 ± 0.1	0.5 ± 0.1	37 ± 7	171 ± 34	5.0 ± 1.0	79 ± 16
JK-Blank	4.8 ± 1.0	0.5 ± 0.1	3.2 ± 0.6	37 ± 7	182 ± 36	1.5 ± 0.3	86 ± 17
JK-1	2 ± 0.4	0.8 ± 0.2	0.9 ± 0.2	86 ± 17	177 ± 35	4.1 ± 0.8	127 ± 25
JK-2	1.6 ± 0.3	1 ± 0.2	0.7 ± 0.1	67 ± 13	232 ± 46	3.9 ± 0.8	118 ± 24
JK-3	2 ± 0.4	2.4 ± 0.5	1.5 ± 0.3	133 ± 27	412 ± 82	11 ± 2	223 ± 45
JK-4	2 ± 0.4	0.8 ± 0.2	0.4 ± 0.1	44 ± 9	155 ± 31	3.5 ± 0.7	80 ± 16
CB-Blank2	3 ± 0.6	1.1 ± 0.0	3.7 ± 0.7	67 ± 13	189 ± 38	3.1 ± 0.6	116 ± 23
CB-1	3 ± 0.6	0.6 ± 0.1	0.9 ± 0.2	66 ± 13	128 ± 26	6.9 ± 1.4	99 ± 20
CB-2	1.8 ± 0.4	0.4 ± 0.1	0.6 ± 0.1	47 ± 9	165 ± 33	3.7 ± 0.7	85 ± 17
CB-3	1.3 ± 0.3	0.4 ± 0.1	0.5 ± 0.1	40 ± 8	122 ± 24	4.5 ± 0.9	68 ± 13
CB-5	0.2 ± 0.0	0.9 ± 0.2	0.7 ± 0.1	20 ± 4	94 ± 19	2.0 ± 0.4	41 ± 8
CB-6	0.1 ± 0.0	0.3 ± 0.1	0.5 ± 0.1	16 ± 3	92 ± 18	<1	35 ± 7
CB-6–reheat	1.3 ± 0.3	0.8 ± 0.2	0.8 ± 0.2	47 ± 9	150 ± 30	2.7 ± 0.5	81 ± 16
CB-7	0.1 ± 0.0	0.4 ± 0.1	0.6 ± 0.1	20 ± 4	111 ± 22	<1	43 ± 9
CB-Blank2	1.3 ± 0.3	0	0	13 ± 3	50 ± 10	<1	25 ± 5

*Calculated using the following equation: $2 \times BSW + MSW + TBDMS\text{-}F + MePro + 1/5 \times CH_4$.